

The effect of hydrothermal treatment on samaria and gadolinia doped ceria powders synthesized by coprecipitation

Alexander Rodrigo Arakaki ^{1,a}, Walter Kenji Yoshito ^{1,b}, Valter Ussui ^{1,c},
Dolores Ribeiro Ricci Lazar ^{1,d}

¹Instituto de Pesquisas Energéticas e Nucleares – Av. Prof. Lineu Prestes, 2242
Cidade Universitária, SP, SP, Brasil

^aalexander@ipen.br, ^bwyoshito@ipen.br, ^cvussui@ipen.br, ^ddrlazar@ipen.br

Keywords: Doped-ceria, synthesis, coprecipitation, hydrothermal treatment

Abstract. One of the main applications of ceria-based (CeO_2) ceramics is the manufacturing of Intermediate Temperature Solid Oxide Fuel Cells electrolytes. In order to improve ionic conductivity and densification of these materials various powder synthesis routes have been studied. In this work powders with composition $\text{Ce}_{0.8}(\text{SmGd})_{0.2}\text{O}_{1.9}$ have been synthesized by coprecipitation and hydrothermal treatment. A concentrate of rare earths containing 90wt% of CeO_2 and other containing 51% of Sm_2O_3 and 30% of Gd_2O_3 , both prepared from monazite processing, were used as precursor materials. The powders were characterized by X-ray diffraction, scanning and transmission electron microscopy, agglomerate size distribution by laser scattering and specific surface area by gas adsorption. Ceramic sinterability was evaluated by dilatometry and density measurements by Archimedes method. High specific surface area powders ($\sim 100\text{m}^2/\text{g}$) and cubic fluorite structure were obtained after hydrothermal treatment around 200°C . Ceramic densification was improved when compared to the one prepared from powders calcined at 800°C .

Introduction

Ceria (CeO_2) has many applications and is widely used in solid oxide fuel cells (SOFC), polishing agents, catalysts, gas sensors, luminous materials, and ceramic pigments. Rare earth doped ceria has high ionic conductivity at relatively low temperatures. This property allows its use as Solid Oxide Fuel Cell electrolyte, being the most promising material [1-3].

Several types of wet-chemical methods have been reported for the synthesis of doped ceria. These include oxalate[4], hydroxide[5] and carbonate[6] coprecipitation, sol-gel[7], combustion[8], hydrothermal and solvothermal treatment [9-19]. The hydrothermal process has attracted a lot of attention due to the possibility of production of nanoparticles of different sizes and shapes, like nanorods[9,10], nanotubes[10-12], nanowires[13], dendrites[14], nanocubes[15,16], nanograins[17], spherical crystallites[18] and triangular microplates[19]. For this purpose parameters like pH of precursors solution, reaction temperature, reaction time, solute concentration and type of solvent have to be controlled. Hydrothermal synthesis has been considered to be a superior method for low-cost production of ceramic powders because of low temperatures involved during processing. In this work powders with composition $\text{Ce}_{0.8}(\text{SmGd})_{0.2}\text{O}_{1.9}$ have been synthesized by coprecipitation followed by hydrothermal treatment, in order to replace the calcination process.

Materials and Methods

A concentrate of rare earths containing 90wt% of CeO_2 and other containing 51% of Sm_2O_3 and 30% of Gd_2O_3 , both prepared from monazite processing, were used as starting materials. The reagents were mixed and diluted in water to achieve a solution containing $35\text{g}\cdot\text{L}^{-1}$ of oxides with $\text{Ce}_{0.8}(\text{SmGd})_{0.2}\text{O}_{1.9}$ stoichiometry. Solution pH was adjusted to 1.0 with ammonia, and dropwise

added to a stirred ammonia solution 7.0M to proceed the coprecipitation. The obtained gels were submitted to the following treatments:

Procedure 1. Washing with water and hydrothermal ageing at 200°C for 4, 8 and 16h under autogenous pressure with stirring (Parr Instruments, 4566 Mini Reactor). The supernatants were filtered and the precipitates were dried at 80°C for 24 h, and codified 2H200-4/8/16. The ceramic powders 2H200-4 and 2H200-8 were ball milled for 15h in ethanol and dried at 80°C for 24 h, becoming 2H200-4MB and 2H200-8MB.

Procedure 2. Washing with water, ethanol and butanol, treatment by azeotropic distillation with butanol and hydrothermal ageing at 200°C for 16h. This powders, codified 2H200-16A, was submitted to ball milling (2H200-16-AMB) and high-energy milling (2H200-16-AMA).

Procedure 3. For comparison purposes coprecipitated gel submitted to ethanol washing, azeotropic distillation and drying (sample 1H80) was also characterized. After calcination at 800°C for 1 hour to oxide crystallization, this powder was codified as 1H-800.

The resulting powders were pressed by uniaxial compaction at 100MPa in a metallic matrix. The green pressed pellets were sintered in air at 1400 and 1500°C for 1 h using an electrical box furnace (Lindberg/Blue M). The powders were characterized by X-ray diffraction (*Rigaku, Multiflex*), scanning and transmission electron microscopy (*Philips, XL30 and JEOL, JEM 2100, respectively*), agglomerate size distribution by laser scattering (*CILAS, 1064*), thermal analysis (TG/DTA) (*Setaram Labsys Instrumentation, TG-DTA/DSC*) and specific surface area by gas adsorption (B.E.T.) (*Quantachrome, Nova 1200*). Ceramic sinterability was evaluated by dilatometry (*Setaram Labsys Instrumentation, TMA*) and density measurements by Archimedes method.

Results and Discussions

XRD patterns of $\text{Ce}_{0.8}(\text{SmGd})_{0.2}\text{O}_{1.9}$ powders after the hydrothermal treatment (Fig.1) show the crystallization of ceria fluorite phases structure (JCPDS-34-394) with increasing time of treatment. This result indicates the possibility of crystallization at low temperatures (200°C) under autogenous pressure. It is also observed that sample obtained without hydrothermal treatment (1H80) has low crystallinity.

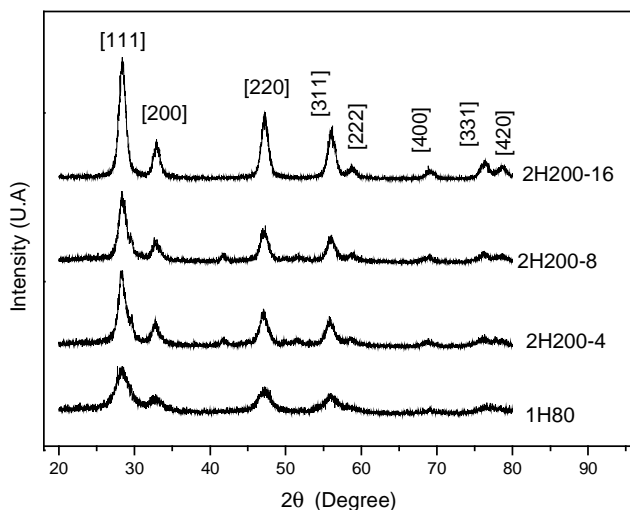


Figure 1. X-ray diffraction patterns of $\text{Ce}_{0.8}(\text{SmGd})_{0.2}\text{O}_{1.9}$ synthesized powders.

The particle size distribution curves presented in Fig. 2 show the lowest mean agglomerate for milled powders. It is worth noting the increase of agglomerate average size with increase of time of hydrothermal treatment.

SEM micrographs (Fig.3), show the influence of the hydrothermal treatment time on the agglomerates growth. The comparison of Fig.3a and 3b indicates that 4 hours of hydrothermal treatment does not promotes agglomerate growth. Increasing the time, the agglomerate size increase simultaneously to the crystallinity.

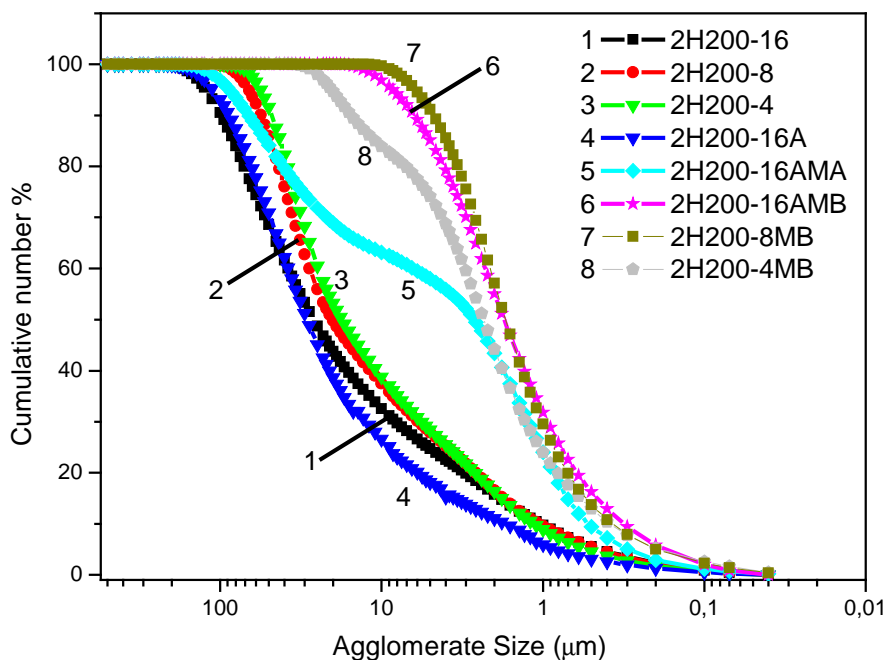


Figure 2. Agglomerate size distribution curves of $Ce_{0.8}(SmGd)_{0.2}O_{1.9}$ synthesized powders.

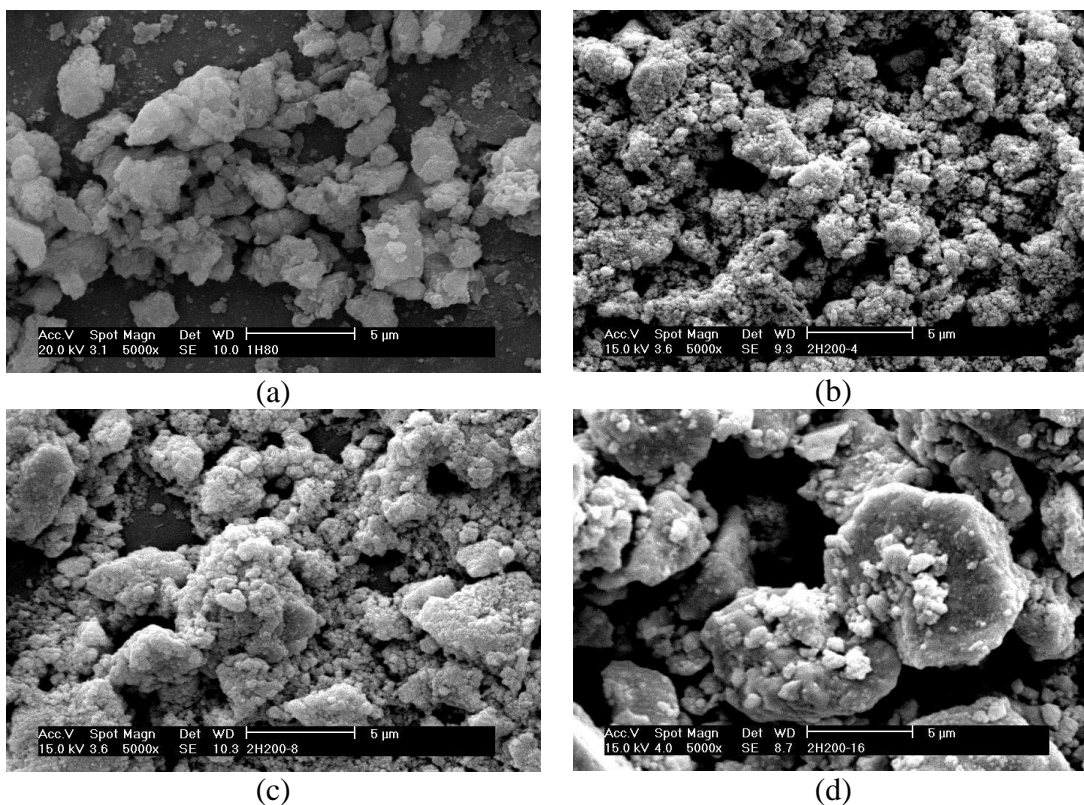


Figure 3. SEM micrographs of $Ce_{0.8}(SmGd)_{0.2}O_{1.9}$ synthesized powders: (a) 1H80, (b) 2H200-4, (c) 2H200-8 and (d) 2H200-16.

Specific surface area values of prepared powders are presented in Table 1. It can be observed that all the powders have high reactivity (around $100m^2.g^{-1}$), but the inclusion of azeotropic distillation step before hydrothermal ageing (procedure 2) increase this parameter. This result indicates that despite agglomerate growth, particle size is in nanometer scale. TEM micrograph of 2H-200-16 sample (Fig.4) confirms this statement.

Table 1. Specific surface area values of $Ce_{0.8}(SmGd)_{0.2}O_{1.9}$ synthesized powders.

Sample code	Specific surface area (m^2/g)	Sample code	Specific surface area (m^2/g)
1H80	223.72		
2H200-4	94.34	2H200-16	107.50
2H200-4MB	94.36	2H200-16-A	114.84
2H200-8	103.41	2H200-16-AMA	117.05
2H200-8MB	96.88	2H200-16-AMB	113.93

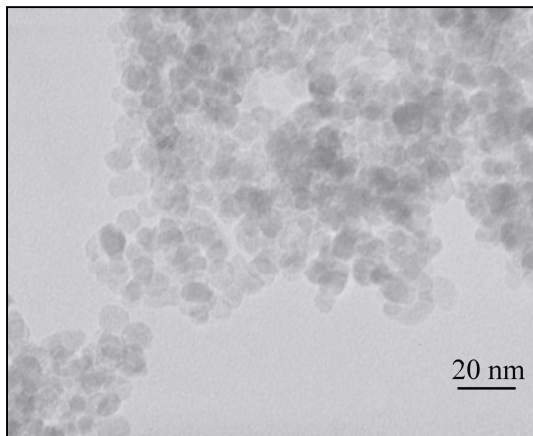


Figure 4. TEM micrograph of $Ce_{0.8}(SmGd)_{0.2}O_{1.9}$ synthesized powder (code 2H200-16)

The TG/DTA results of the thermal decomposition process of sample 2H200-16 is shown in Fig.5. The weight loss around 11% is due to the remain removal of OH^- groups of hydrated oxide. Endothermic peak are produced by the weight loss up to $100^\circ C$. Exothermic peak corresponds to the improvement of oxide crystallization and the oxidation of Ce^{3+} [5]. Powders treated for 4 and 8 hours had the same behaviour.

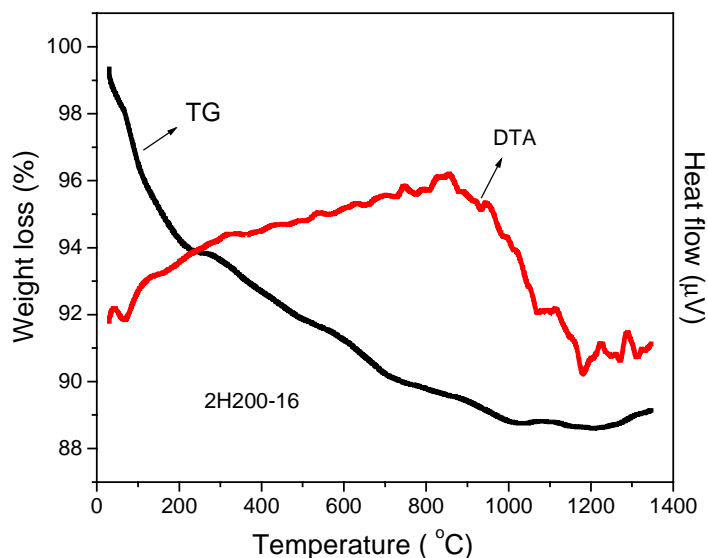


Figure 5. DTA/TG analysis of $Ce_{0.8}(SmGd)_{0.2}O_{1.9}$ synthesized powder (code 2H200-16)

Sintering behaviour of the compacted powders in air under a constant heating rate of $10^\circ C/min$ is shown in Fig. 6. Two shrinkage mechanisms is observed: The first one from room temperature until $1100^\circ C$ may be related to the remain loss of OH^- groups. Above this temperature a continuous

shrinkage is observed due sintering processes. The full densification was not reached due to equipment limit temperature. The maximum shrinkage rate is observed near 1400°C and based upon this result, 1400°C and 1500°C were selected as the sintering temperatures to obtain dense ceramics under isothermal conditions.

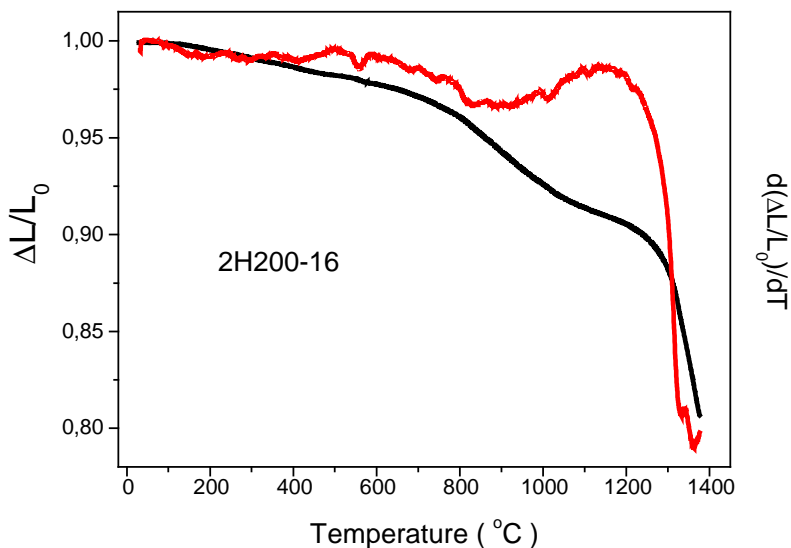


Figure 6. Linear shrinkage and linear shrinkage rate of green pellet of $Ce_{0.8}(SmGd)_{0.2}O_{1.9}$ powder (code 2H200-16), as a function of sintering temperature.

Table 2 show the relative density of green and sintered $Ce_{0.8}(SmGd)_{0.2}O_{1.9}$ pellets, determined by geometric and Archimedes method, respectively, and considering $7.2g.cm^{-3}$ as the theoretical density. It can be observed that the powder 2H200-4 and 2H200-8 provided the highest density (>96%DT). This is explained by the small size of agglomerate, that enabled better densification during the sintering. Milling processes and the employment of azeotropic distillation with butanol before the hydrothermal treatment were not effective to improve density. Comparison with relative density values of sintered sample prepared from coprecipitated powders submitted to calcining and milling (1H-800) show that hydrothermal treatment is an effective process for reduction of sintering temperature.

Table 2. Relative density of the $Ce_{0.8}(SmGd)_{0.2}O_{1.9}$ pellets.

Sample code	Relative green density (% pt)*	Relative sintered density (% pt)*	
		Temperature (°C)	
		1400	1500
2H200-4	33.1	96.0	96.4
2H200-4MB	33.6	94.8	95.6
2H200-8	32.3	95.7	96.4
2H200-8MB	34.3	91.6	93.8
2H200-16	37.4	89.2	90.5
2H200-16-AMA	36.9	90.5	93.1
2H200-16-AMB	37.2	89.1	93.2
1H-800	32.8	87.5	95.4

*Theoretical density of $7.2g.cm^{-3}$ [20]

Conclusions

Hydroxide coprecipitation synthesis followed by hydrothermal ageing demonstrated to be a promising route for production of ceria – samaria – gadolinia nanometer powders. Crystallization can be improved and high specific surface area values (around $100 \text{ m}^2 \cdot \text{g}^{-1}$) can be reached. Despite the high state of agglomeration of powders, high density ceramics are obtained by sintering at 1400°C , which is an improvement compared to the use of powders crystallized by calcining. In order to reduce the formation of hard agglomerates solvothermal treatments with various organic solvents will be performed.

Acknowledgments

The authors would like to thank the CNPq (Project 471491/2007-1) and FINEP (PaCOS network) for the financial support and the scholarship. Thanks also to our colleagues from CCTM/IPEN and PROCEL/IPEN, especially from the Laboratories of Microscopy, XRD, Cilas and Thermal Analysis.

References

- [1] S.M Haile, *Acta Mater.*, Vol.51 (2003), p.5981.
- [2] D. Z. Florio, F. C. Fonseca, E. N. S. Muccillo; R. Muccillo, *Cerâmica*, Vol.50 (2004), p.275.
- [3] A. Abrão, *Química e Tecnologia das Terras-Raras*. CETEM/CNPq – Série Tecnologia Mineral nº66. Rio de Janeiro, RJ.(1994).
- [4] K. Higashi, K. Sonoda, H. Ono; S. Sameshima, Y. Hirata, *J. Mater. Res.* Vol.14, n.3 (1999), p. 957.
- [5] B. Djuricic, S. Pickering, *J. Eur. Ceram. Soc.* Vol.19 (1999), p.1925.
- [6] J.G. Li, T. Ikegami, Y. Wang, T. Mori, *J. Am. Ceram. Soc.* Vol. 85, n. 9 (2002), p. 2376.
- [7] W. Huang, P. Shuk, M. Greenblatt, *Solid State Ionics* Vol.100 (1997), p.23.
- [8] T. Mahata, G. Das; R. K. Mishra, B. P. Sharma, *J. Alloys Compd.* Vol.391 (2005), p.129.
- [9] A.Vantomme, Z.Y.Yuan; G. Du; B.L. Su, *Langmuir* Vol.21, n. 3 (2005), p.1132.
- [10] C. Pan, D. Zhang, L. Shi, *J. Solid State Chem.*, Vol.181 (2008), p. 1298.
- [11] D. Zhang, H. Fu, L. Shi, J. Fang, Q. J. Li, *Solid State Chem.*, Vol. 180 (2007), p.654.
- [12] K. Zhou, Z. Yang, S. Yang, *Chem. Mater.* Vol.19 (2007), p. 1215.
- [13] Q. Yuan, H. H. Duan; L.D. Sun, Y.W. Zhang, C. H. J. Yan, *J. Colloid. Interf. Sci.* Vol. 335 (2009), p.151.
- [14] M. Wu, Q. Zhang, Y. Liu, Q. Fang, X. Liu, *Mater. Res. Bull.* Vol.44 (2009), p.1437.
- [15] Z. Yang, Y. Yang, H. Liang, L. Liu, *Mater. Lett.* Vol.63 (2009), p.1774.
- [16] A. A. Atwale, M.S. Bapat, P. A. Desai, *J. Alloys Compd.*, 2009, in press.
- [17] M. S. Tsai, *Mat. Lett.* Vol.58 (2004), p.2270.
- [18] F. Zhou, X. Ni, Y. Zhang, H. Zheng, *J. Colloid Interface Sci.* Vol.307 (2007), p.135.
- [19] Z. Guo, F. Du, G. Li; Z. Cui, *Inorg. Chem.* Vol.45 (2006), p.4167.
- [20] M. Mogensen, N. M. Sammes; G. A. Tompsett, *Solid State Ionics* Vol.129 (2000), p.63-94.